Phytochemistry 85 (2013) 185–193

Contents lists available at SciVerse ScienceDirect

Phytochemistry

journal homepage: www.elsevier.com/locate/phytochem

Characterization of chlorinated valepotriates from *Valeriana jatamansi*

Sheng Lin [a,b,1], Zhong-Xiao Zhang [a,1], Tao Chen [c], Ji Ye [a], Wei-Xing Dai [a], Lei Shan [a], Juan Su [a], Yun-Heng Shen [a], Hui-Liang Li [a], Run-Hui Liu [a], Xi-ke Xu [a], Hui Wang [c,*], Wei-dong Zhang [a,*]

[a] *Department of Natural Product Chemistry, School of Pharmacy, Second Military Medical University, 325 Guohe Road, Shanghai 200433, People's Republic of China*
[b] *State Key Laboratory of Bioactive Substance and Function of Natural Medicines, Institute of Materia Medica Chinese Academy of Medical Sciences and Peking Union Medical College, Beijing 100050, People's Republic of China*
[c] *Key Laboratory of Nutrition and Metabolism, Institute for Nutritional Sciences, Shanghai Institutes for Biological Sciences, Chinese Academy of Sciences and Graduate School of the Chinese Academy of Sciences, Shanghai 200031, People's Republic of China*

ARTICLE INFO

Article history:
Received 6 April 2012
Received in revised form 26 June 2012
Available online 1 October 2012

Keywords:
Valeriana jatamansi
Valerianaceae
Chlorinated valepotriates
Dereplication
Cytotoxicity

ABSTRACT

HPLC–PDA–MS and TLC analysis were used to look for minor cytotoxic chlorinated valepotriates from whole plants of *Valeriana jatamansi* (syn. *Valeriana wallichii* DC.). This resulted in isolation of 15 chlorinated valepotriates, designated as chlorovaltrates A-O, together with six known analogues, (1*S*,3*R*,5*R*,7*S*,8*S*,9*S*)-3,8-epoxy-1,5-dihydroxyvalechlorine, volvaltrate B, chlorovaltrate, rupesin B, (1*S*,3*R*,5*R*,7*S*,8*S*,9*S*)-3,8-epoxy-1-*O*-ethyl-5-hydroxyvalechlorine, and (1*R*,3*R*,5*R*,7*S*,8*S*,9*S*)-3,8-epoxy-1-*O*-ethyl-5-hydroxyvalechlorine. Their structures were elucidated by spectroscopic methods including homo- and heteronuclear two-dimensional NMR experiments. Chlorovaltrates K-N, chlorovaltrate and rupesin B showed moderate cytotoxicity against lung adenocarcinoma (A 549), metastatic prostate cancer (PC-3M), colon cancer (HCT-8) and hepatoma (Bel 7402) cell lines with IC_{50} values of 0.89–9.76 μM.

1. Introduction

Natural products continue to play an important role in the discovery and development of new chemical entities as drug-lead compounds (Cragg et al., 1997; Newman et al., 2003; Newman and Cragg, 2007). The remaining major challenge in the isolation and purification of bioactive natural products is the efficient detection of a desired class of compounds. Although bioactivity-directed fractionation is effective, it is usually problematic when multiple, potentially interfering active or nonspecifically active compounds are present. Dereplication, the rapid identification of known compounds present in a mixture, is crucial to the fast discovery of novel natural products. Dereplication processes typically combine chromatographic and spectroscopic methods with database searching. A hyphenated technique of HPLC coupled to UV photodiode array detection (HPLC/UV) and to mass spectrometry (HPLC/MS or HPLC/MS^n) has been extensively used as effective tool for the online identification of natural products in plant extract analysis (Gao et al., 2010; Stobiecki et al., 2010; Li et al., 2006). The advantage of this method is that minor components can be identified in the presence of major metabolites of bioactive fractions. For example, a desired class of compounds, such as the halogenated secondary metabolites, could be readily located in the fractions by HPLC–MS analysis due to their characteristic MS isotope patterns (Oh et al., 2006; Chlipala et al., 2010; Allard et al., 2012).

Valepotriates, a family of iridoid esters exhibiting a variety of properties of biological significance, have been attracting great interest in natural products. Phytochemical studies on the plants of the genus *Valeriana* (Valerianaceae) have resulted in a series of valepotriates, some of which showed potent cytotoxic and antitumor activities (Stahi and Schütz, 1980; Tang et al., 2002; Yu et al., 2005; Becker et al., 1984; Bounthanh et al., 1981). A recent investigation of *Valeriana jatamansi* (syn. *Valeriana wallichii* DC.) led to the isolation of 29 previously unreported iridoids and 17 known ones, including four chlorinated valepotriates (Lin et al., 2009, 2010a,b). Interestingly, the major chlorinated valepotriate, volvaltrate B (**17**), induced a significant percentage of definitive remissions of ovarian tumors in the female mice (Zhang et al., 2010). This thus extended our attention to the chlorinated valepotriates of *V. jatamansi*. A large-scale extract of *V. jatamansi* (25 kg) was then undertaken to enrich the minor chlorinated valepotriates. Application of bioactivity-directed fractionation combined with HPLC–PDA–MS and TLC analysis has resulted in discovery of fifteen minor chlorinated valepotriates (**1–15**) and six known analogues. Reported herein are the isolation, structure elucidation, and biological activities of the isolates.

* Corresponding authors. Tel.: +86 21 54920941; fax: +86 21 54920291 (H. Wang), tel./fax: +86 21 81871244 (W.-d. Zhang).
E-mail addresses: huiwang@sibs.ac.cn (H. Wang), wdzhangy@hotmail.com (W.-d. Zhang).
[1] These authors have contributed equally to this work.

0031-9422/$ - see front matter © 2012 Elsevier Ltd. All rights reserved.
http://dx.doi.org/10.1016/j.phytochem.2012.08.015

2. Results and discussion

2.1. Biological and chemical screening of the minor chlorinated valepotriates from the whole plants of V. jatamansi

In previous work, LC/(±)ESI-MS analysis of chlorinated valepotriates showed typical isotopic patterns for monochlorinated secondary metabolites ($[M + Na]^+$:$[M + Na + 2]^+$ = 3:1, $[M + Cl]^-$:$[M + Cl + 2]^-$ = 3:2). In particular, using TLC ($CHCl_3$–MeOH, 20:1), the chlorinated valepotriates displayed a characteristic green colored spot on spraying with 10% H_2SO_4 reagent followed by heating. The fractionation and isolation procedures were then guided by LC/UV, LC/ESI-MS/MS, TLC, and cytotoxic assays (Table 1 and Section 4). The subfraction C_3 had the greatest cytotoxic activity among the C subfractions of the EtOAc fraction. However, after removing the major compounds volvaltrate B and IVHD-valtrate, the residue (fraction $C_{3\text{-}2}$) of subfraction C_3 still retained the hightest cytotoxic activity. Thus, fraction C_{3-2} was selected for further analysis by HPLC-DAD/ESIMS^n to obtain detailed structural information (Figs. 1 and 2 and Figures S1–S17 in Supplementary Information). The constituents of this subfraction were tentatively characterized based on their retention times, UV spectra, and MS^n fragmentation information (Table 3). It was evident from HPLC-MS profile of the fraction C_{3-2} that monochloriated compounds were present, because at least 20 components contained distinct peaks with monochloriated isotope patterns. Correspondingly, TLC analysis of fraction C_{3-2} showed at least five minor spots under UV light that turned green, with a series of other green and reddish brown spots (non-chlorinated valepotriates), on spraying with 10% H_2SO_4 reagent and heating. These results guided the targeted isolation of the chlorinated valepotriates in fraction C_{3-2}. HPLC-DAD analysis indicated that the UV spectra of peaks 14 and 17–20 exhibited two broad maximum absorption bands at λ 200 and 250–260 nm, which were characteristic for the presence of diene valepotriates. On the other hand, the UV spectra ($\lambda_{max} \sim 204$ nm) of peaks 1–13, 15 and 16 indicated the presence of monoene valepotriates (Fig. 3). These characteristic UV spectra can be used to differentiate between diene and monoene valepotriates. Moreover, all 20 peaks except for peaks 1–3, and 5 yielded a fragment ion at *m/z* 102 or *m/z* 204 in the positive MS^2 mode, which was characteristic for the loss of one or two isovaleroxy units (Figures S1–S17, Supplementary Information). Therefore, peaks 4, and 6–21 could be characterized as monoene and diene chlorinated valepotriates containing one or two isovaleroxy units, while peaks 1–3, and 5 could be elucidated as monoene chlorinated valepotriates with no isovaleroxy units. Peaks 1–3, and 13 were readily assigned as (1*S*,3*R*,5*R*,7*S*,8*S*,9*S*)-3,8-epoxy-1,5-dihydroxyvalechlorine (**16**), (1*S*,3*R*,5*R*,7*S*,8*S*,9*S*)-3,8-epoxy-1-*O*-ethyl-5-hydroxyvalechlorine, (1*R*,3*R*,5*R*,7*S*,8*S*,9*S*)-3,8-epoxy-1-*O*-ethyl-5-hydroxyvalechlorine, and volvaltrate B (**17**), respectively, by comparing their retention times with those of authentic samples in HPLC experiments and their R_f values in TLC analysis.

Analysis of the literature showed that only four chlorinated valepotriates, rupesins A-C and chlorovaltrate, have been previously reported from the other Valerianaceae species (Yang et al., 2006; Fuzzati et al., 1996). However, only peak 19 possessed the same molecular weight as rupesin B or chlorovaltrate. These suggested that at least fifteen chlorinated valepotriates present in *V. jatamansi* should be new. Targeted isolation of these chlorinated valepotriates by HP-20 macroporous adsorbent resin, ODS, Sephadex LH-20, preparative TLC, and preparative HPLC led to identification of fifteen new chlorinated valepotriates, chlorovaltrates AO (**1**–**15**), and two known ones, chlorovaltrate (**18**) and rupesin B (**19**).

Table 1
Cytotoxicity of the various fractions of the whole plants of *V. jatamansi*.

Fraction	IC_{50} (μg mL^{-1})			
	A 549	PC-3M	HCT-8	Bel 7402
Alcohol extract	22.3	18.8	29.4	25.2
EtOAc fraction	16.3	12.2	15.8	12.1
Fr. A	>50	48.1	42.3	>50
Fr. B	38.1	25.4	31.2	41.4
Fr. C	12.6	7.8.	11.5	12.0
Fr. D	23.4	18.9	21.1	16.7
Fr. C_1	38.4	25.3	41.2	>50
Fr. C_2	6.9	6.1	8.2	6.4
Fr. C_3	6.3	6.8	7.6	6.1
Fr. C_{3-2}	5.2	4.6	6.1	4.8
Fr. C_4	13.4	15.8	21.7	25.4
Fr. C_5	18.6	28.4.	19.5	16.6

Table 2
Cytotoxicity of Compounds **1**–**15**, **18** and **19** to A 549, PC-3M, HCT-8, and Bel 7402 cell lines.

Compound	IC_{50} (μM)			
	A 549	PC-3M	HCT-8	Bel 7402
1	>10	>10	>10	>10
2	>10	>10	>10	>10
3	>10	>10	>10	>10
4	>10	>10	>10	>10
5	6.58	4.92	7.15	4.56
6	4.27	2.34	4.22	2.35
7	>10	3.48	2.71	>10
8	>10	6.25	9.51	>10
9	>10	7.16	8.62	>10
10	7.52	3.69	6.02	>10
11	3.17	2.04	2.90	2.35
12	8.26	3.83	2.32	7.23
13	9.76	4.79	1.93	2.70
14	4.70	1.06	0.89	2.11
15	>10	6.25	9.51	>10
18	5.70	2.59	3.28	3.54
19	3.71	2.24	1.41	2.03
PAB[a]	0.39	1.54	1.63	1.16

[a] Pseudolaric acid B was used as a positive control.

2.2. Structure elucidation of obtained constituents

Chlorovaltrate A (**1**) was obtained from peak 7 and gave a molecular formula of $C_{17}H_{23}ClO_7$ on the basis of HRESIMS and NMR spectroscopic data. Its IR, ^{1}H and ^{13}C NMR spectra are similar to those of (1*S*,3*R*,5*R*,7*S*,8*R*,9*S*)-3,8-epoxy-1,5-dihydroxyvalechlorine (**16**) except for the presence of an isovaleroxy substituent (δ_C 170.7, 43.2, 25.7, 22.3 and 22.2) (Lin et al., 2010a). Online LC-DAD/MS^n analyses suggested the presence of one isovaleroxy group in **1** (Figure S1, Supplementary Information). This substituent was readily assigned at C-1 since the signal for H-1 was significantly deshielded due to the acylation effect. Further proof that the isovaleroxy group was attached to C-1 was provided by an HMBC correlation from H-1 to the carbonyl carbon at $_C$ 170.7. Based on biogenetic considerations, chlorovaltrate A (**1**) was assumed to possess the same absolute configuration as in **16**. Therefore, **1** was elucidated as (1*S*,3*S*,5*R*,7*S*,8*S*,9*S*)-3,8-epoxy-5-hydroxy-1-isovaleroxyvalechlorine.

Chlorovaltrate B (**2**), corresponding to peak 4, was deduced as $C_{18}H_{27}ClO_8$ from its HRESIMS. This formula required 5° of unsaturation, one less than that of chlorovaltrate A (**1**). Analysis of the ^{1}H and ^{13}C NMR spectroscopic data (Tables 4 and 6) showed resonances similar to those of **1**, but also indicated that the oxo bridge connecting C-3 and C-8 had been converted to 3-methoxy and 8-hydroxy functionalities, and this appeared to explain the 32 Da mass reduction found between the two compounds. HMBC correlation from methoxy protons to C-3 and no observed correlation be-

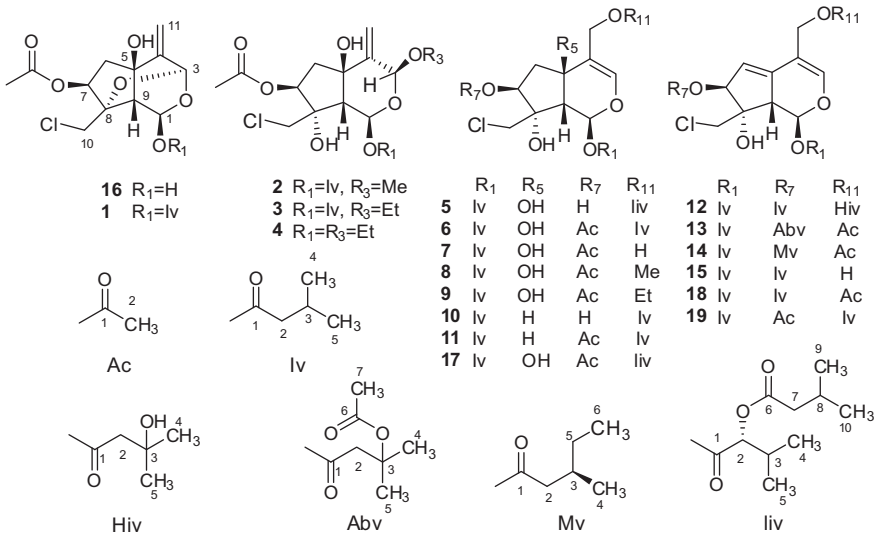

	R_1	R_5	R_7	R_{11}
5	Iv	OH	H	Iiv
6	Iv	OH	Ac	Iv
7	Iv	OH	Ac	H
8	Iv	OH	Ac	Me
9	Iv	OH	Ac	Et
10	Iv	H	H	Iv
11	Iv	H	Ac	Iv
17	Iv	OH	Ac	Iiv

	R_1	R_7	R_{11}
12	Iv	Iv	Hiv
13	Iv	Abv	Ac
14	Iv	Mv	Ac
15	Iv	Iv	H
18	Iv	Iv	Ac
19	Iv	Ac	Iv

Fig. 1. Compounds **1**–**19**.

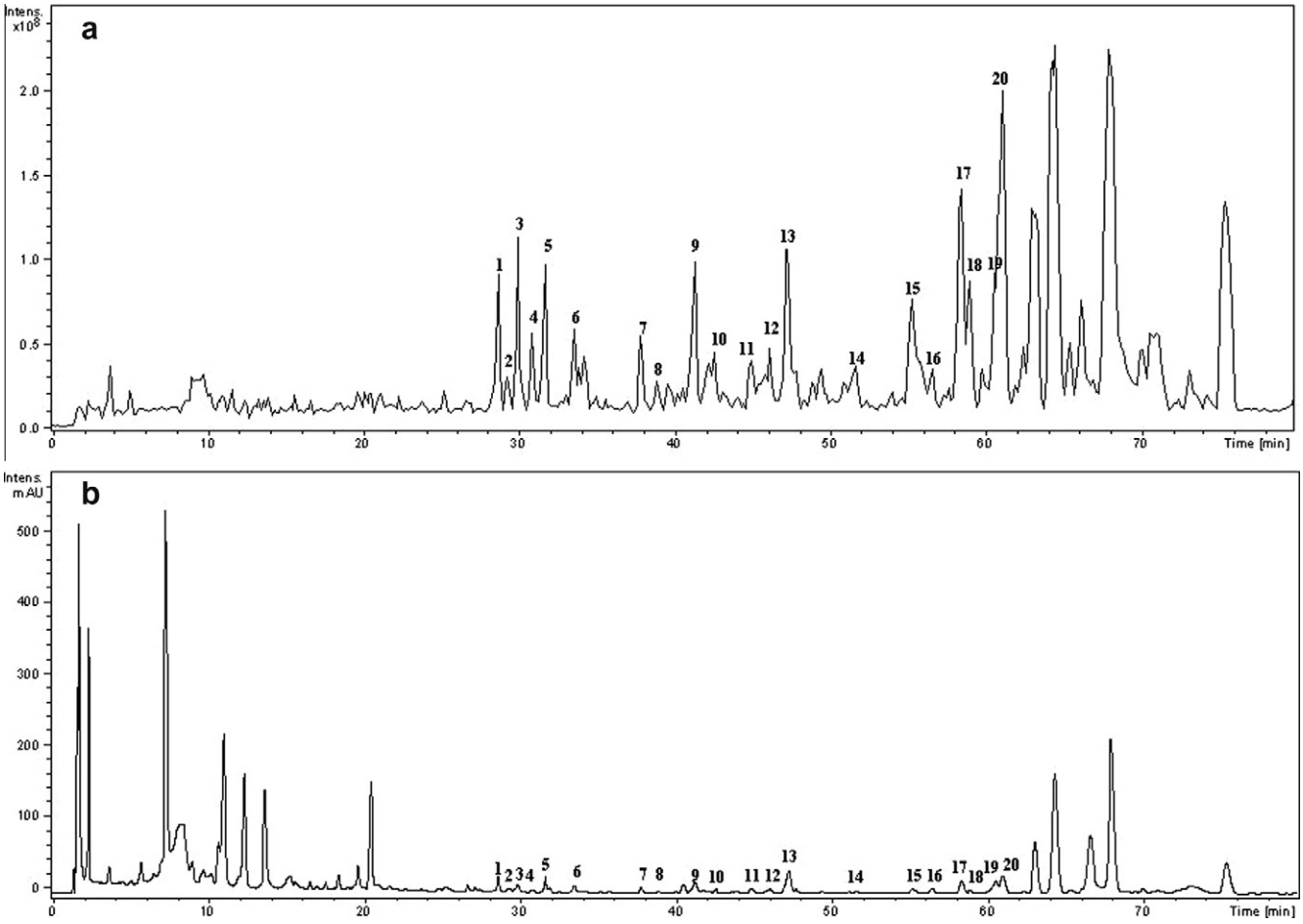

Fig. 2. HPLC/ESIMS^n analysis of the cytotoxic fraction C_3 from *V. jatamansi*: (a) total ion chromatogram, all mass (b) UV chromatogram (λ = 204 nm).

tween H-3 and C-8 supported the deduction. The relative configuration of **2** was assigned by analysis of NOESY NMR spectroscopic data. Analogous correlations from protons on the cyclopentane ring confirmed that **2** has the same configuration as **1** at C-5, C-7, C-8, and C-9. NOESY correlations from H-3 to H-6α and H-1 indicated that these protons, opposite of H-9 and *MeO*-3, were spatially close on the same face of the tetrahydro-*2H*-pyran ring (Figure S29, Supporting Information). On the basis of these data and biogenetic considerations, **2** was assigned as (1*S*,3*R*,5*R*,7*S*,8*S*,9*S*)-5,8-dihydroxy-3-methoxy-1-isovaleroxyvalechlorine.

Chlorovaltrate C (**3**) from peak 6 was an analogue of **2**. Comparison of the NMR and MS data between **2** and **3**

Table 3
MS characteristics of compounds from fraction $C_{3\text{-}2}$ of *V. jatamansi*.

Peak (t_R, min)	Compounds	$[M + Na]^+$, *m/z*	$[M + Cl]^-$, *m/z*	HPLC/ESIMS^n, *m/z* (Positive mode)	Monoene/diene form shown by UV
4 (30.8)	**2**	429	441	MS^2, 327, 291	Monoene
5 (31.6)	**4**	387	399	MS^2, 351, 305, 245	Monoene
6 (33.5)	**3**	443	455	MS^2, 341, 305	Monoene
7 (37.8)	**1**	397	409	MS^2, 295	Monoene
8 (38.5)	**5**	557	569	MS^2, 355, 253, 235	Monoene
9 (41.3)	**7**	415	427	MS^2, 379, 313, 295, 213, 177	Monoene
10 (42.1)	**10**	441	453	MS^2, 339, 237	Monoene
11 (44.8)	**8**	429	441	MS^2, 393, 327, 295, 227, 191	Monoene
12 (46.0)	**9**	443	455	MS^2, 407, 341, 295, 241, 205	Monoene
13 (47.2)	**17**	599	611	MS^2, 397, 295	Monoene
14 (51.4)	**15**	439	451	MS^2, 337, 235, 213, 177	Diene
15 (54.9)	**6**	499	511	MS^2, 397, 295, 217	Monoene
16 (56.4)	**11**	483	495	MS^2, 381	Monoene
17 (58.2)	**12**	539	551	MS^2, 465, 335, 277	Diene
18 (58.6)	**14**	495	507	MS^2, 277, 219	Diene
19 (60.5)	**18**, **19**	481	–	MS^2, 379, 319, 277, 219	Diene
20 (60.8)	**13**	539	551	MS^2, 437, 379, 277, 219	Diene

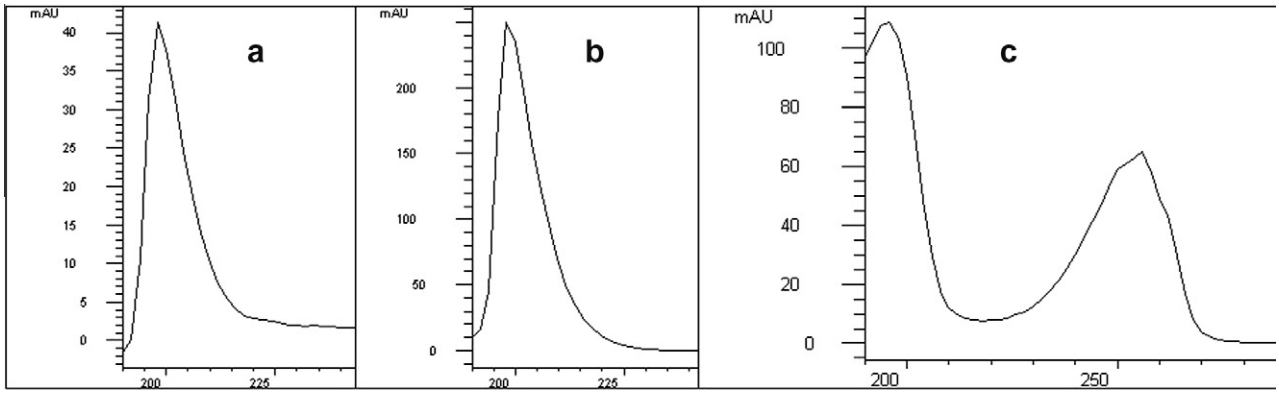

Fig. 3. Characteristic UV spectra for monoene chlorinated valepotriates ($\Delta^{4,11}$, a; $\Delta^{3,4}$, b) and diene chlorinated valepotriates (c).

demonstrated that the only difference was replacement of resonances for OMe in **2** by those for OEt in **3**. Accordingly, **3** was established as (1*S*,3*R*,5*R*,7*S*,8*S*,9*S*)-5,8-dihydroxy-3-ethoxy-1-isovaleroxyvalechlorine.

Chlorovaltrate D (**4**) from peak 5 was inferred as $C_{16}H_{25}ClO_7$ by HRESIMS. Analysis of ^1H and ^{13}C NMR data suggested that chlorovaltrate D (**4**) had the same iridoid nucleus as chlorovaltrate B (**2**), but lacked the resonances corresponding to the isovaleroxy and *O*-methyl units and instead contained two *O*-ethyl groups at C-1 and C-3, respectively. Further interpretation of 2D NMR spectroscopic data allowed structure **4** to be assigned. NOESY NMR experiments with **4** displayed identical correlations to those observed in **2** and **3**. Hence, **4** was identified as (1*S*,3*R*,5*R*,7*S*,8*S*,9*S*)-1,3-diethoxy-5,8-dihydroxyvalechlorine.

Chlorovaltrate E (**5**) from peak 8 was analyzed for $C_{25}H_{39}ClO_{10}$ by HRESIMS and NMR spectroscopic data. Since the NMR spectra of **5** showed the absence of one acetyl signal, it was clear that compound **5** was the deacetyl analogue of volvaltrate B (**17**) (Tables 4 and 6). As expected, H-7 of **5** was significantly shifted upfield due to the deacylation effect when compared with the ^1H NMR spectroscopic data of **17** (Table 4). Thus, chlorovaltrate E (**5**) was assigned as the 7-*O*-deacetyl derivative of **17**, which was confirmed by the detailed 2D NMR experiments and negative $[\alpha]_D^{20}$ value of **5**. Thus, **5** was deduced as (1*S*,5*R*,7*S*,8*S*,9*S*)-10-chloro-5,7-dihydroxy-11-[(*R*)-α-(isovaleroxy)isovaleroxy]-1-isovaleroxy-5,6-dihydrovaltrate chlorohydrin.

Chlorovaltrate F (**6**) from peak 15 gave a molecular formula of $C_{22}H_{33}ClO_9$ on the basis of HRESIMS. The NMR spectroscopic features of **6** were similar to those of volvaltrate B (**17**), except for the presence of one (*R*)-α-isovaleroxyisovaleroxy group instead of an isovaleroxy group at C-11 in **6** (Tables 4 and 6). Further interpretation of the 2D NMR spectroscopic data of **6** confirmed this assignment and completed the full assignments the ^1H and ^{13}C NMR signals. Therefore, **6** was determined as (1*S*,5*R*,7*S*,8*S*,9*S*)-7-acetoxy-10-chloro-5-hydroxy-1,11-diisovaleroxy-5,6-dihydrovaltrate chlorohydrin.

Chlorovaltrate G (**7**) from peak 9 was found to possess the molecular formula, $C_{17}H_{25}ClO_8$, as shown from its HRESIMS. The ^1H and ^{13}C NMR spectroscopic data (Tables 4 and 6) showed signals similar to those of **6**, but H_2-11 was significantly shielded and one isovaleryl group was absent. These spectroscopic differences suggested that chlorovaltrate G (**7**) was an 11-*O*-deisovaleryl derivative of **6**. The 2D NMR spectroscopic data were also consistent with those observed for **7**. Thus, **7** was assigned to be (1*S*,5*R*,7*S*,8*S*,9*S*)-7-acetoxy-10-chloro-5,11-dihydroxy-1-isovaleroxy-5,6-dihydrovaltrate chlorohydrin.

Chlorovaltrate H (**8**) from peak 11 was assigned the molecular formula of $C_{18}H_{27}ClO_8$ by HRESIMS. The ^1H and ^{13}C NMR spectroscopic data of **8** closely resembled those of **6** except that 11-isovaleroxy group was replaced by a methoxy unit [δ_H 3.37 (3H, s); δ_C58.2]. This was supported by the downfield shift of C-11 from δ_C 71.4 in **8** to δ_C 61.3 in **6**, as well as by gHSQC and gHMBC experiments of **8**. Consequently, **8** was proposed to be (1*S*,5*R*,7*S*,8*S*,9*S*)-7-acetoxy-10-chloro-5-hydroxy-1-isovaleroxy-11-methoxy-5,6-dihydrovaltrate chlorohydrin.

Chlorovaltrate I (**9**) from peak 12 was assigned as the 11-*O*-ethyl derivative of **7** by comparison of the NMR and MS data between **7**, **8** and **9** (Tables 4–6). Hence, **9** was defined as

Table 4
^{1}H NMR spectroscopic data (δ) for compounds **1**–**8**.[a]

	No.	**1** ($CDCl_3$)	**2** ($CDCl_3$)	**3** ($CDCl_3$)	**4** (Me_2CO-d_6)	**5** ($CDCl_3$)	**6** ($CDCl_3$)	**7** (Me_2CO-d_6)	**8** ($CDCl_3$)
	1	6.43 d (3.6)	6.25 d (2.4)	6.26 d (6.0)	5.02 d (3.6)	6.33 d (4.8)	6.55 d (1.8)	6.45 d (2.4)	6.50 d (1.2)
	3	5.34 s	5.20 s	5.31 s	5.29 s	6.55 s	6.54 s	6.34 s	6.39 s
	6	2.61 dd (13.8, 7.2)	2.70 dd (14.4, 6.0)	2.88 dd (15.0, 6.0)	2.57 dd (15.0, 7.2)	2.41 dd (13.8, 4.2)	2.58 dd (13.2, 6.0)	2.61 dd (13.8, 5.4)	2.58 dd (13.8, 6.0)
		2.06 dd (13.8, 2.4)	2.04 dd (14.4, 6.0)	2.01 dd (15.0, 2. 4)	1.84 dd (15.0, 6. 0)	2.10 dd (13.8, 4.2)	2.11 dd (13.2, 7.2)	2.06 dd (13.8, 6.0)	2.10 dd (13.8, 5.4)
	7	4.98 dd (7.2, 2.4)	5.03 dd (6.0, 6.0)	5.13 dd (6.0, 2.4)	5.15 dd (7.2, 6.0)	4.03 dd (4.2, 4.2)	4.92 dd (6.0, 7.2)	4.96 dd (5.4, 6.0)	4.89 dd (6.0, 5.4)
	9	2.67 d (3.6)	2.57 d (2.4)	2.52 d (6.0)	2.42 d (3.6)	2.59 d (4.8)	2.71 d (1.8)	2.65 d (2.4)	2.68 d (1.2)
	10	3.82 d (11.4)	3.86 d (11.4)	3.85 d (11.4)	4.08 d (11.4)	4.11 d (11.4)	3.77 d (11.4)	3.94 d (11.4)	3.84 d (11.4)
		3.79 d (11.4)	3.77 d (11.4)	3.81 d (11.4)	3.96 d (11.4)	3.80 d (11.4)	3.70 d (11.4)	3.90 d (11.4)	3.74 d (11.4)
	11	5.42 s	5.45 s	5.49 s	5.34 s	4.81 d (12.0)	4.75 d (12.6)	4.31 brd (12.6)	4.18 d (12.0)
		5.16 s	5.39 s	5.36 s	5.29 s	4.75 d (12.0)	4.67 d (12.6)	4.17 brd (12.6)	3.91 d (12.0)
R_1	2	2.20 m	2.22 m	2.22 m	3.84 m, 3.45 m	2.20 m	2.23 m[b]	2.21 m	2.25 m
	3	2.09 m	2.11 m	2.10 m	1.13 t (6.6)	2.10 m	2.10 m	2.08 m	2.11 m
	4	0.96 d (6.6)[b]	0.96 d (6.6)[b]	0.96 d (6.6)[b]		0.98 d (6.6)[b]	0.98 d (6.6)[c]	0.96 d (6.6)	0.97 d (6.6)
	5	0.95 d (6.6)[b]	0.95 d (6.6)[b]	0.95 d (6.6)[b]		0.97 d (6.6)[b]	0.97 d (6.6)[c]	0.96 d (6.6)	0.97 d (6.6)
R_7	2	2.09 s	2.10 s	2.09 s	2.04 s		2.11 s	2.06 s	2.09 s
R_{11}	2					4.75 d (4.8)	2.22 m[b]		
	3					2.23 m	2.10 m		
	4					1.01 d (7.2)[c]	0.98 d (6.6)[c]		
	5					1.00 d (7.2)[c]	0.97 d (6.6)[c]		
	7					2.28 m			
	8					2.10 m			
	9					0.98 d (6.6)[b]			
	10					0.97 d (6.6)[b]			
	OMe/ OEt		3.50 s	/3.96 m, 3.57 m; 1.25 t (6.6)	/3.93 m, 3.59 m; 1.22 t (6.6)				3.37 s

[a] ^{1}H NMR data () were measured in 600 MHz NMR instrument. Proton coupling constants (J) in Hz are given in parentheses. The assignments were based on DEPT, ^{1}H–^{1}H COSY, NOESY, HSQC, and HMBC experiments.
[b,c] Assignment may be interchanged in each column.

(1*S*,5*R*,7*S*,8*S*,9*S*)-7-acetoxy-10-chloro-11-ethoxy-5-hydroxy-1-isovaleroxy-5,6-dihydrovaltrate chlorohydrin.

Chlorovaltrate J (**10**) from peak 10 was determined to be the 5,6-dihydrovaltrate chlorohydrin valepotriate with two isovaleroxy groups from its spectroscopic data and 2D NMR data analysis. The two isovaleroxy groups were located at C-1 and C-11 by the HMBC correlations from H-1 and H_2-11 to the corresponding carbonyl carbon signals at δ_C 171.4 and 173.0, respectively. The configuration of **10** was identical with that of didrovaltrate acetoxy hydrin on the basis of the NOE correlation of H-5/H-9/H_2-10 and the coupling constant (9.6 Hz) between H-5 and H-9 and the negative $[\alpha]_D^{20}$ value. Accordingly, **10** was assigned as (1*S*,5*S*,7*S*,8*S*,9*S*)-10-chloro-7-hydroxy-1,11-diisovaleroxy-5,6-dihydrovaltrate chlorohydrin.

Spectroscopic analysis of chlorovaltrate J (**11**) from peak 16 indicated that it is an acetyl derivative of **10** due to the presence of an acetyl unit in **11** (Tables 5 and 6). This was supported by its molecular formula, showing 58 Da more than that of **10**. The relatively downfield proton chemical shift for H-7 in **11** compared to H-7 in **10** suggested that **11** was the 7-*O*-acetyl derivative of **10**. Therefore, **11** was determined as (1*S*,5*S*,7*S*,8*S*,9*S*)-7-acetoxy-10-chloro-1,11-diisovaleroxy-5,6-dihydrovaltrate chlorohydrin.

The molecular formula of chlorovaltrate K (**12**) from peak 17 was inferred as $C_{25}H_{37}ClO_9$ by HRESIMS. The ^{1}H NMR spectrum displayed characteristics of a valtrate chlorohydrin nucleus (Lin et al., 2009), exhibiting signals for two olefinic methines [δ_H 6.85 (s, H-3) and 5.81 (dd, J = 3.0, 2.4 Hz, H-6)] and an oxymethylene [δ_H 4.81 and 4.70 (each 1H, J = 12.6 Hz, H_2-11)]. Characteristic resonances for three acyloxy moieties found in **12**, including two isovaleroxy groups and a 3-hydroxyisovaleroxy moiety, were observed in the ^{1}H, ^{13}C, and DEPT NMR spectra. Further 2D NMR data analysis allowed the three acyloxy moieties to be positioned at C-1, C-7, and C-11, respectively. In the NOESY spectrum, the observed NOESY correlations between H-9 and H_2-10 and between H-7 and *OH*-8 indicated that **12** has the same configuration as **6** at C-1, C-7, C-8 and C-9. Hence, **12** was deduced as (1*S*,7*S*,8*S*,9*S*)-10-chloro-11-(3-hydroxyisovaleroxy)-1,7-diisovaleroxyvaltrate chlorohydrin.

Chlorovaltrate M (**13**) from peak 20 was formulated as $C_{24}H_{33}ClO_{10}$ from HRESIMS. The ^{1}H and ^{13}C NMR spectra indicated that chlorovaltrate M (**13**) possessed the same iridoid nucleus as **12**. Three acyloxy substituents were readily assigned as an isovaleroxy, a β-(acetoxy)isovaleroxy, and an acetoxy group by analysis of the ^{1}H and ^{13}C NMR spectroscopic data of **13** (Tables 5 and 6). Finally, the observed HMBC correlations from H-1, H-7 and H_2-11 to the respective carbonyl carbon signals at δ_C 170.5, 168.9, and 170.8 served to locate the three acyloxy substituents at C-1, C-7 and C-11, respectively. Thus, **13** was defined as (1*S*,7*S*,8*S*,9*S*)-11-acetoxy-7-[β-(acetoxy)isovaleroxy]-10-chloro-1-isovaleroxyvaltrate chlorohydrin.

Chlorovaltrate N (**14**) from peak 18 was established the molecular formula $C_{23}H_{33}ClO_8$ by its HRESIMS. The ^{1}H and ^{13}C NMR spectra of chlorovaltrate N (**14**) were very similar to those of **13**, with the same iridoid nucleus and 1-isovaleroxy and 11-acetoxy again present; however, two methyls at δ 0.88 (3H, t, J = 7.2 Hz) and 0.93 (3H, d, J = 6.6 Hz) in the ^{1}H NMR spectrum of **14** indicated the presence of a 3-methylvaleroxy residue in place of the β-(acetoxy)isovaleroxy at C-7 in **14**. The ^{13}C and 2D NMR data closely matched those observed for **14** and confirmed the position of the 3-methylvaleroxy group at C-7. The absolute configuration of 3-methylvaleroxy in **14** was determined by basic hydrolysis. Basic hydrolysis of **14** yielded 3-methylvaleric acid (Section 4). Comparison of the optical rotation data of 3-methylvaleric acid {$[\alpha]_D^{20}$ − 6.3(c 0.15, CH_2Cl_2)} and (*R*)-3-methylvaleric acid $[\alpha]_D^{25}$ − 8.4 (c 1.0, CH_2Cl_2)} demonstrated the *R* configuration of the 3-methylvaleric acid (Belzecki et al., 2000). Therefore, **14** was determined as (1*S*,7*S*,8*S*,9*S*)-11-acetoxy-10-chloro-1-isovaleroxy-7-[(*R*)-3-methylvaleroxy]-valtrate chlorohydrin.

Table 5
^{1}H NMR spectroscopic data (δ) for compounds **9–15.**[a]

	No.	**9** (Me_2CO-d_6)	**10** (Me_2CO-d_6)	**11** ($CDCl_3$)	**12** (Me_2CO-d_6)	**13** ($CDCl_3$)	**14** (Me_2CO-d_6)	**15** (Me_2CO-d_6)
	1	6.46 d (1.8)	6.14 d (6.0)	6.19 d (5.4)	6.21 d (9.6)	6.24 d (10.8)	6.21d (9.6)	6.17 d (10.8)
	3	6.37 s	6.46 s	6.46 s	6.85 s	6.67 s	6.83 s	6.65 s
	5		3.05 m	2.93 m				
	6	2.61 dd (13.8, 6.0)	2.04 m	2.24 m	5.81 dd (3.0, 2.4)	5.76 dd (2.4, 2.4)	5.79 dd (2.4, 2.4)	5.80 dd (3.0, 2.4)
		2.02 dd (13.8, 5.4)	1.97 m	2.10 m				
	7	4.97 dd (6.0, 5.4)	4.08 brd (2.4)	5.02 dd (4.2, 3.6)	5.49 d (3.0)	5.42 d (2.4)	5.49 d (2.4)	5.48 d (3.0)
	9	2.66 d (1.8)	2.39 dd (9.6, 6.0)	2.91 dd (9.6, 5.4)	3.00 dd (9.6, 2.4)	2.91 dd (10.8, 2.4)	3.01 dd (9.6, 2.4)	2.96 dd (10.8, 2.4)
	10	3.94 d (11.4)	4.04 d (11.4)	3.84 d (11.4)	4.08 d (11.4)	3.98 d (11.4)	4.09 d (11.4)	4.07 d (11.4)
		3.90 d (11.4)	3.80 d (11.4)	3.73 d (11.4)	3.86 d (11.4)	3.78 d (11.4)	3.87 d (11.4)	3.86 d (11.4)
	11	4.13 d (12.0)	4.62 d (12.0)	4.61 d (12.0)	4.81 d (12.6)	4.70 d (12.0)	4.75 d (12.0)	4.22 s
		4.04 d (12.0)	4.44 d (12.0)	4.43 d (12.0)	4.70 d (12.6)	4.62 d (12.0)	4.66 d (12.0)	4.21 s
R_1	2	2.21 m	2.23 m[b]	2.19 m[b]	2.38 m	2.29 m	2.37 m	2.37 m
	3	2.08 m	2.08 m[c]	2.10 m[c]	2.13 m	2.15 m	2.13 m	2.13 m
	4	0.94 d (6.6)[b]	0.98 d (6.6)[d]	0.96 d (6.6)[d]	1.00 d (6.6)[b]	1.00 d (6.6)	1.00 d (6.6)	1.00 d (6.6)
	5	0.93 d (6.6)[b]	0.97 d (6.6)[d]	0.95 d (6.6)[d]	0.99 d (6.6)[b]	1.00 d (6.6)	1.00 d (6.6)	1.00 d (6.6)
R_7	2	2.05 s		2.07 s	2.19 (m)	3.01 d (14.4)	2.30 m, 2.13 m	2.19 (m)
						2.81 d (14.4)		
	3				2.08 (m)		1.87 m	2.08 (m)
	4				0.96 d (6.6)[b]	1.50 s[b]	1.39 m, 1.22 m	0.96 d (6.6)[b]
	5				0.95 d (6.6)[b]	1.53 s[b]	0.88 t (7.2)	0.94 d (6.6)[b]
	6					1.95 s	0.93 d (6.6)	
R_{11}	2		2.17 m[b]	2.17 m[b]	2.45 s	2.04 s	1.98 s	
	3		2.07 m[c]	2.07 m[c]				
	4		0.96 d (6.6)[d]	0.96 d (6.6)[d]	1.24 s			
	5		0.95 d (6.6)[d]	0.95 d (6.6)[d]	1.24 s			
	OEt	3.51 m, 1.15 t (7.2)						

[a] ^{1}H NMR data () were measured in 600 MHz NMR instrument. Proton coupling constants (J) in Hz are given in parentheses. The assignments were based on DEPT, ^{1}H–^{1}H COSY, NOESY, HSQC, and HMBC experiments.
[b,c,d] Assignment may be interchanged in each column.

Table 6
^{13}C NMR spectroscopic data (δ) for compounds **1–15, 18** and **19.**

	No.	**1**[a]	**2**[a]	**3**[a]	**4**[b]	**5**[a,c]	**6**[a]	**7**[b]	**8**[a]	**9**[b]	**10**[b]	**11**[a]	**12**[b]	**13**[a]	**14**[b]	**15**[b]	**18**[a]	**19**[a]
	1	89.5	89.9	89.0	98.2	90.8	89.3	90.4	89.5	90.4	91.2	89.4	93.5	92.3	93.5	93.5	92.4	92.4
	3	94.4	101.0	99.2	99.1	144.5	143.1	139.4	140.6	140.7	141.2	141.0	148.9	148.1	148.8	145.8	148.0	148.0
	4	151.0	142.5	145.4	148.7	114.8	113.6	119.2	114.5	116.3	115.5	113.0	110.2	108.6	110.3	115.1	108.7	108.8
	5	77.5	76.1	79.1	78.8	75.4	70.9	72.7	71.9	72.2	33.8	32.7	140.5	139.5	140.5	141.1	139.3	139.5
	6	46.5	40.3	43.7	43.7	43.8	41.0	43.0	42.3	43.1	38.6	35.0	118.6	117.1	118.5	117.9	117.4	117.2
	7	74.0	79.4	80.4	80.9	78.2	79.8	80.1	79.8	80.1	77.8	80.0	83.6	83.3	83.6	83.9	83.2	83.5
	8	83.1	81.2	82.5	83.0	83.0	80.3	81.8	80.9	81.8	83.9	81.8	81.5	80.2	81.5	81.4	80.3	80.3
	9	45.5	57.5	58.8	60.5	55.6	54.4	55.9	53.9	55.8	46.2	45.4	50.5	49.3	50.5	50.7	49.3	49.3
	10	45.2	49.1	49.5	51.6	50.5	49.6	50.9	49.5	51.0	50.8	49.1	49.4	48.4	49.4	49.5	48.4	48.5
	11	108.9	114.1	114.8	110.9	62.6	61.3	60.8	71.4	69.0	64.1	63.3	61.3	60.8	61.4	59.5	60.9	60.5
R_1	1	170.7	171.5	171.2	64.3	171.0	171.8	170.7	171.6	170.6	171.4	171.1	171.1	170.5	171.1	171.1	170.5	170.5
	2	43.2	43.4	43.7	15.8	43.4	43.4[d]	43.7	43.4	43.7	43.9	43.4[d]	43.6	43.2	44.0	44.0	43.4[d]	43.4[d]
	3	25.7	25.4	25.7		25.9	25.7	26.3	25.8	26.3	26.5	25.7	26.4	25.7	26.4	26.4	25.7[e]	25.7
	4	22.3	22.4	22.6		22.6	22.4	22.6	22.6	22.6	22.7	22.4[e]	22.8[d]	22.3[d]	22.6[d]	22.7[d]	22.4[f]	22.4[e]
	5	22.2	22.4	22.6		22.6	22.4	22.6	22.6	22.6	22.7	22.3[e]	22.7[d]	22.2[d]	22.5[d]	22.6[d]	22.3[f]	22.3[e]
R_7	1	169.5	170.5	170.0			170.8	171.8	171.0	171.7		169.8	172.1	168.9	172.3	172.1	171.8	169.7
	2	21.0	21.0	21.3			20.9	21.0	21.2	21.0		21.0	44.0	44.2	43.6	43.6	43.5[d]	21.0
	3												26.4	79.3	32.8[e]	26.4	25.8[e]	
	4												22.6[d]	26.6[e]	30.5[e]	22.6[d]	22.4[f]	
	5												22.5[d]	26.5[e]	11.6	22.5[d]	22.3[f]	
	6													170.4	19.6			
	7													22.2				
R_{11}	1						173.0				173.0	172.9	172.3	170.8	171.0		170.8	172.9
	2						43.2[d]				43.9	43.3[d]	48.3	20.9	20.9		20.9	43.2[d]
	3						25.7				26.5	25.7	69.5					25.7
	4						22.4				22.7	22.4[e]	29.9					22.4[e]
	5						22.4				22.7	22.3[e]	29.9					22.3[e]
	OMe/ OEt		55.9	/64.8, 15.1	/64.8, 15.9				58.2	65.8, 15.5								

[a] ^{13}C NMR data () were measured in $CDCl_3$ for **1–3**, **5**, **6**, **8**, **11**, **13**, **18** and **19** at 150 MHz. The assignments were based on DEPT, ^{1}H–^{1}H COSY, HSQC, and HMBC experiments.
[b] ^{13}C NMR data () were measured in acetone-d_6 for **4**, **7**, **9**, **10**, **12**, **14** and **15** at 150 MHz. The assignments were based on DEPT, ^{1}H–^{1}H COSY, HSQC, and HMBC experiments.
[c] Data of the α-isovaleroxyisovaleroxy group at C-11 of **5**: δ 170.0 ($C_{R11\text{-}1}$), 77.1 ($C_{R11\text{-}2}$), 30.3 ($C_{R11\text{-}3}$), 19.0 ($C_{R11\text{-}4}$), 17.6 ($C_{R11\text{-}5}$), 173.6 ($C_{R11\text{-}6}$), 43.3 ($C_{R11\text{-}7}$), 25.9 ($C_{R11\text{-}8}$), 22.6 ($C_{R11\text{-}9}$), 22.5 ($C_{R11\text{-}10}$).
[d,e,f] Assignment may be interchanged in each column.

The molecular formula of chlorovaltrate L (**15**) from peak 14 was found to be $C_{20}H_{29}ClO_7$ on the basis of HRESIMS. In comparison with data from **12**, the ^{1}H NMR, ^{13}C NMR, and mass spectroscopic data established the lack of a 3-hydroxyisovaleryl moiety

in **15**. Furthermore, the relatively upfield proton chemical shift for H_2-11 in **15** compared to H_2-11 in **12** suggested that the loss of the 3-hydroxyisovaleryl moiety from *OH*-11, leaving two isovaleroxy groups to be located at C-1 and C-7, respectively. This conclusion was supported by analysis of 2D NMR data. Thus, **15** was established as (1*S*,7*S*,8*S*,9*S*)-10-chloro-11-hydroxy-1,7-diisovaleroxyvaltrate chlorohydrin.

The known compounds **18** and **19** from peak 19 were identified as chlorovaltrate and rupesin B, respectively, by comparing the UV, MS, and NMR data with those reported in the literature and analyzing their 2D NMR data (Yang et al., 2006; Fuzzati et al., 1996; Becker et al., 1984).

Although compounds **6**, **8**, and **11** have been presented in separated patents, no spectroscopic data have been reported (Thies and David, 1983; Zhang et al., 2009). By using the MTT method compounds **1–15**, **18** and **19** were tested *in vitro* against several human cancer cell lines including lung adenocarcinoma (A 549), metastatic prostate cancer (PC-3M), colon cancer (HCT-8) and hepatoma (Bel 7402) cell lines, and pseudolaric acid B was used as a positive control (Lin et al., 2009). Compounds **11–14**, **18** and **19** showed moderate cytotoxicity against all tested cell lines with IC_{50} values of 0.89–9.76 μM. Except for compounds **14** the remaining compounds exhibited selective cytotoxicity against metastatic prostate cancer (PC-3M) cell line with IC_{50} values of 0.89–9.51 μM (Table 2).

3. Conclusion

Target isolation of minor chlorinated valepotriates from the whole plants of *V. jatamansi* was conducted by application of bioactivity-directed fractionation combined with dereplication principle. This resulted in the fast discovery of fifteen chlorinated valepotriates (**1–15**) and six known analogues, most of which exhibited cytotoxicity against A 549, PC-3M, HCT-8 and Bel 7402 cell lines with IC_{50} values of 0.89–9.76 μM. With such an approach, the time-consuming isolation of common natural products is avoided and the success rate of discovering new and/or bioactive compounds is increased dramatically.

4. Experimental

4.1. General experimental procedures

Optical rotations were measured on a Perkin-Elmer 341 polarimeter. IR and UV spectra were recorded on a Bruker Vector-22 and Shimadzu UV-2550 UV–visible spectrophotometers, respectively. NMR spectra were acquired on a Bruker Avance 600 MHz or Avance 300 MHz NMR spectrometer in $CDCl_3$ or Me_2CO-d_6 with TMS as an internal standard. ESIMS and HRESIMS were acquired on an Agilent LC/MSD Trap XCT and a Q-TOF micro mass spectrometer (Waters, USA), respectively. Column chromatography (CC) was performed using silica gel (100–200, 300–400 mesh, and 10–40 μm; Huiyou Silical Gel Development Co. Ltd., Yantai, PR China) and Sephadex LH-20 (40–70 μm; Amersham Pharmacia Biotech AB, Uppsala, Sweden). Semipreparative HPLC was conducted on an ODS column (Kromasil, 5 μm, 300 × 10 mm) using a PDA UV detector at 208 nm. Preparative TLC (0.4–0.5 mm) was performed on precoated silica gel GF_{254} plates (Yantai). Zones were visualized under UV light (254 nm) or by spraying with 10% H_2SO_4 followed by heating.

4.2. Plant material

Whole plants of *V. jatamansi* were collected in Gaopo, Guizhou Province, PR China, in July 2009, and identified by Prof. Shun-zhi He in Guiyang University of Traditional Chinese Medicine. A herbarium specimen was deposited in School of Pharmacy, Second Military Medical University, PR China (herbarium No. 2009–03-1).

4.3. HPLC-DAD/ESIMS^n Analyses of Constituents in Fractions

For online HPLC-DAD/ESIMS^n analyses, an Agilent 1100 Series liquid chromatography system chromatography was utilized equipped with a quaternary pump, degasser, column oven, autosampler, and diode array detector operating at 204 and 254 nm, which was coupled to MSD Trap XCT ESI mass spectrometer. The positive ion ESIMS^n experiments were conducted using conditions as follows: drying temperature, 350 °C; drying gas (N2), 10 L/min; nebulizer gas, high-purity nitrogen (N_2), 35 psi; collision gas, ultra-high-purity helium (He); skimmer, 40 V; injection rate, 5.0 μL/min. HPLC separation performed on an Eclipse C18 XDB column (4.6 × 150 mm, 5 μm) using a mobile phase of MeOH and H_2O (flow rate, 0.8 mL/min; temperature, 25 °C). The mobile phase gradient program was 10:90 (t = 0 min), 60:40 (t = 40 min), 95: 5 (t = 70 min), and 95:5 (t = 80 min). Each fractions (2.0 mg) was dissolved in MeOH (1 mL), filtered through a 0.45 μm microporous membrane, and stored at 4 °C until analysis.

4.4. Extraction and isolation

The extraction and isolation procedures were guided by LC-MS screening and cytotoxic assays. The air-dried whole plants of *V. jatamansi* (25 kg) were powdered and extracted with EtOH–H_2O, (40.0 L & 95:5, v/v) at room temperature for 3 × 48 h. The EtOH extract was evaporated under reduced pressure to yield a residue (2640 g). The residue was suspended in H_2O (2000 mL) and then partitioned with EtOAc (5 × 2000 mL). The EtOAc fraction (1050 g) was applied to a HP-20 macroporous adsorbent resin column. Successive elution of the column with EtOH–H_2O (1:9, 3:7. 7.3 & 95:5) (5000 mL each) yielded four fractions (A–D, 125, 286, 319, and 168 g, respectively) after removing the solvents. A portion of cytotoxic fraction C (300 g) was separated by Sephadex LH-20 CC eluting with MeOH to give five subfractions (C_1–C_5), which were subjected to the cytotoxic assay. Subfractions C_2 (55 g) and C_3 (61 g) showed significant cytotoxicity. Subfraction C_2 mainly contained volvaltrate B (**17**) and IVHD-valtrate by TLC analysis. However, after removing volvaltrate B (**17**) and IVHD-valtrate by CC over Sephadex LH-20 eluting with MeOH, the residue (fraction $C_{3-2,}$ 42 g) of subfraction C_3 still remained the highest cytotoxic activity. HPLC-MS^n and TLC analysis of fraction C_{3-2} indicated that fraction C_{3-2} was rich in chlorinated valepotriates. A portion of subfraction C_{3-2} (35 g) was then separated by medium-pressure liquid chromatography over reversed-phase silica gel eluting with a gradient of increasing MeOH (10–100%) in H_2O to give ten fractions (C_{3-2-1}–C_{3-2-10}). Subfraction C_{3-2-3} (3.5 g), including mainly peaks 1–6 was fractioned by CC over Sephadex LH-20 using $CHCl_3$–MeOH (1:1) to afford six subfractions ($C_{3-2-3-1}$–$C_{3-2-3-6}$). Subfraction $C_{3-2-3-2}$ (125 mg) was separated by reversed-phase preparative HPLC (RP_{18}, 5 μm, 25010 mm, 208 nm, MeCN–H_2O, 45:55) to give **2** (6.2 mg) and **3** (5.8 mg), respectively. Subfractions $C_{3-2-3-3}$ and $C_{3-2-3-4}$ mainly contained **16**, (1*S*,3*R*,5*R*,7*S*,8*S*,9*S*)-3,8-epoxy-1-*O*-ethyl-5-hydroxyvalechlorine, and (1*R*,3*R*,5*R*,7*S*,8*S*,9*S*)-3,8-epoxy-1-*O*-ethyl-5-hydroxyvalechlorine, respectively. Subfraction $C_{3-2-3-5}$ (160 mg) was separated by reversed-phase preparative HPLC (RP_{18}, 5 μm, 250 × 10 mm, 208 nm, MeCN–H_2O, 42:58) to give **4** (13.2 mg). Subfraction C_{3-2-4} (346 mg), mainly consisting of peaks 7 and 8, was isolated after preparative TLC developed with $CHCl_3$–MeOH (20:1) and then reversed-phase preparative HPLC (RP18, 5 μm, 208 nm, MeCN–H_2O, 45:55) to give **1** (10.3 mg) and **5** (2.8 mg). Subfraction C_{3-2-5} (5.6 g), consisting of peaks 9–12, was separated by CC over Sephadex LH-20 using petroleum ether-CH_3Cl-MeOH (5:5:1) to afford six subfractions

($C_{3-2-5-1}$–$C_{3-2-5-6}$). Subfractions $C_{3-2-5-2}$ (248 mg) and $C_{3-2-5-3}$ (157 mg) were purified by preparative TLC developed with $CHCl_3$–MeOH (20:1) to give **7** (16.2 mg) and **10** (4.1 mg). Separation of subfraction $C_{3-2-5-4}$ (202 mg) by reversed-phase preparative HPLC (RP_{18}, 5 μm, 250 × 10 mm, 208 nm, MeCN–H_2O, 48:52) afforded **8** (7.5 mg) and **9** (8.4 mg). Using the same procedure as described above for the isolation of **1** and **5**, subfractions C_{3-2-6} (1.8 g) yielded a majority of known **17** and a little of **6** (9.0 mg) and **15** (4.2 mg). Subfractions C_{3-2-7} (1.6 g) and C_{3-2-8} (2.8 g) were separated by Sephadex LH-20 CC using petroleum ether–$CHCl_3$–MeOH (5:5:1) and then by reversed-phase preparative HPLC (RP_{18}, 5 μm, 250 × 10 mm, 208 nm, MeCN–H_2O, 55:45) to give **11** (4.6 mg) and **12** (22.5 mg), respectively. Subfraction C_{3-2-9} (6.5 g), including peaks 18–20, was fractioned by Sephadex LH-20 CC using petroleum ether-$CHCl_3$–MeOH (5:5:1) to afford five subfractions ($C_{3-2-9-1}$–$C_{3-2-9-5}$). Subfractions $C_{3-2-9-2}$ (362 mg) and $C_{3-2-9-3}$ (269 mg) were purified by preparative TLC developed with $CHCl_3$–MeOH (20:1) to yield **13** (23.8 mg), **14** (14.6 mg), **18** (6.5 mg) and **19** (5.9 mg), respectively.

4.5. Chlorovaltrate A (1)

Colorless oil, $[\alpha]_D^{20}$ + 79.8 (*c* 0.39, MeOH); UV (MeOH) $_{max}$ (log ε) 204 (3.84) nm; IR (KBr) $_{max}$ 2969, 1738, 1366, 1217, 940 cm^{-1}; for ^1H NMR ($CDCl_3$, 600 MHz) and ^{13}C NMR ($CDCl_3$, 150 MHz) spectroscopic data, see Tables 4 and 6; ESIMS *m*/*z* 397 $[M + Na]^+$ and 409 $[M + Cl]^-$; HRESIMS *m*/*z* 397.1038 $[M + Na]^+$ (calcd for $C_{17}H_{23}ClO_7Na$, 397.1030).

4.6. Chlorovaltrate B (2)

Colorless oil, $[\alpha]_D^{20}$ + 83.5 (*c* 0.31, MeOH); UV (MeOH) $_{max}$ (log ε) 203 (3.82) nm; IR (KBr) $_{max}$ 3447, 2959, 1736, 1373, 1242, 1086, 964 cm^{-1}; for ^1H NMR ($CDCl_3$, 600 MHz) and ^{13}C NMR ($CDCl_3$, 150 MHz) spectroscopic data, see Tables 4 and 6; ESIMS *m*/*z* 429 $[M + Na]^+$, 405 $[M - H]^-$ and 441 $[M + Cl]^-$; HRESIMS *m*/*z* 405.1332 $[M - H]^-$ (calcd for $C_{18}H_{26}ClO_8$, 405.1316).

4.7. Chlorovaltrate C (3)

Colorless oil, $[\alpha]_D^{20}$ + 69.5 (*c* 0.15, MeOH); UV (MeOH) $_{max}$ (log ε) 204 (3.85) nm; IR (KBr) $_{max}$ 2966, 1736, 1368, 1222, 935 cm^{-1}; for ^1H NMR ($CDCl_3$, 600 MHz) and ^{13}C NMR ($CDCl_3$, 150 MHz) spectroscopic data, see Tables 4 and 6; ESIMS *m*/*z* 443 $[M + Na]^+$ and 455 $[M + Cl]^-$; HRESIMS *m*/*z* 443.1165 $[M + Na]^+$ (calcd for $C_{19}H_{29}ClO_8Na$, 443.1449).

4.8. Chlorovaltrate D (4)

Colorless oil, $[\alpha]_D^{20}$ + 100.4 (*c* 0.85, MeOH); UV (MeOH) $_{max}$ (log ε) 204 (3.86) nm; IR (KBr) $_{max}$ 3459, 2977, 1731, 1376, 1245, 1072 cm^{-1}; for ^1H NMR (Me_2CO-d_6, 600 MHz) and ^{13}C NMR (Me_2CO-d_6, 150 MHz) spectroscopic data, see Tables 4 and 6; ESIMS *m*/*z* 387 $[M + Na]^+$ and 399 $[M + Cl]^-$; HRESIMS *m*/*z* 387.1196 $[M + Na]^+$ (calcd for $C_{16}H_{25}ClO_7Na$, 387.1187).

4.9. Chlorovaltrate E (5)

Colorless oil, $[\alpha]_D^{20}$ − 28.0 (*c* 0.16, MeOH); UV (MeOH) $_{max}$ (log ε) 203 (3.92) nm; IR (KBr) $_{max}$ 3467, 2970, 1736, 1367, 1235, 1091 cm^{-1}; for ^1H NMR ($CDCl_3$, 600 MHz) and ^{13}C NMR ($CDCl_3$, 150 MHz) spectroscopic data, see Tables 4 and 6; ESIMS *m*/*z* 557 $[M + Na]^+$ and 569 $[M + Cl]^-$; HRESIMS *m*/*z* 557.2138 $[M + Na]^+$ (calcd for $C_{25}H_{39}ClO_{10}Na$, 557.2129).

4.10. Chlorovaltrate F (6)

Colorless oil, $[\alpha]_D^{20}$ − 76.0 (*c* 0.10, MeOH); UV (MeOH) $_{max}$ (log ε) 204 (3.92) nm; IR (KBr) $_{max}$ 2970, 1738, 1366, 1229, 1217, 1092 cm^{-1}; for ^1H NMR ($CDCl_3$, 600 MHz) and ^{13}C NMR ($CDCl_3$, 150 MHz) spectroscopic data, see Tables 4 and 6; ESIMS *m*/*z* 499 $[M + Na]^+$, 475 $[M - H]^-$and 511 $[M + Cl]^-$; HRESIMS *m*/*z* 499.1722 $[M + Na]^+$ (calcd for $C_{22}H_{33}ClO_9Na$, 499.1711).

4.11. Chlorovaltrate G (7)

Colorless oil, $[\alpha]_D^{20}$ − 39.0 (*c* 0.30, MeOH); UV (MeOH) $_{max}$ (log ε) 203 (3.90) nm; IR (KBr) $_{max}$ 3400, 2969, 1737, 1372, 1231, 1082 cm^{-1}; for ^1H NMR (Me_2CO-d_6, 600 MHz) and ^{13}C NMR (Me_2CO-d_6, 150 MHz) spectroscopic data, see Tables 4 and 6; ESIMS *m*/*z* 415 $[M + Na]^+$, 391 $[M - H]^-$ and 427 $[M + Cl]^-$; HRESIMS *m*/*z* 415.1146 $[M + Na]^+$ (calcd for $C_{17}H_{25}ClO_8Na$, 415.1136).

4.12. Chlorovaltrate H (8)

Colorless oil, $[\alpha]_D^{20}$ − 43.8 (*c* 0.19, MeOH); UV (MeOH) $_{max}$ (log ε) 204 (3.92) nm; IR (KBr) $_{max}$ 3418, 2960, 1734, 1372, 1294, 1082 cm^{-1}; for ^1H NMR ($CDCl_3$, 600 MHz) and ^{13}C NMR ($CDCl_3$, 150 MHz) spectroscopic data, see Tables 4 and 6; ESIMS *m*/*z* 429 $[M + Na]^+$ and 441 $[M + Cl]^-$; HRESIMS *m*/*z* 429.1303 $[M + Na]^+$ (calcd for $C_{18}H_{27}ClO_8$, 429.1292).

4.13. Chlorovaltrate I (9)

Colorless oil, $[\alpha]_D^{20}$ − 49.6 (*c* 0.15, MeOH); UV (MeOH) $_{max}$ (log ε) 204 (3.93) nm; IR (KBr) $_{max}$ 3422, 2962, 1736, 1370, 1292, 1080 cm^{-1}; for ^1H NMR (Me_2CO-d_6, 600 MHz) and ^{13}C NMR (Me_2CO-d_6, 150 MHz) spectroscopic data, see Tables 5 and 6; ESIMS *m*/*z* 443 $[M + Na]^+$ and 455 $[M + Cl]^-$; HRESIMS *m*/*z* 443.1463 $[M + Na]^+$ (calcd for $C_{19}H_{29}ClO_8Na$, 443.1449).

4.14. Chlorovaltrate J (10)

Colorless oil, $[\alpha]_D^{20}$ − 46.0 (*c* 0.27, MeOH); UV (MeOH) $_{max}$ (log ε) 203 (3.92) nm; IR (KBr) $_{max}$ 3489, 2960, 1735, 1370, 1294, 1094 cm^{-1}; for ^1H NMR (Me_2CO-d_6, 600 MHz) and ^{13}C NMR (Me_2CO-d_6, 150 MHz) spectroscopic data, see Tables 5 and 6; ESIMS *m*/*z* 441 $[M + Na]^+$, 417 $[M - H]^-$ and 453 $[M + Cl]^-$; HRESIMS *m*/*z* 441.1670 $[M + Na]^+$ (calcd for $C_{20}H_{31}ClO_7Na$, 441.1656).

4.15. Chlorovaltrate K (11)

Colorless oil, $[\alpha]_D^{20}$ − 57.6 (*c* 0.20, MeOH); UV (MeOH) $_{max}$ (log ε) 203 (3.90) nm; IR (KBr) $_{max}$ 3511, 2962, 1730, 1361, 1314, 1110 cm^{-1};Colorless oil; for ^1H NMR ($CDCl_3$, 600 MHz) and ^{13}C NMR ($CDCl_3$, 150 MHz) spectroscopic data, see Tables 5 and 6; ESIMS *m*/*z* 483 $[M + Na]^+$ and 495 $[M + Cl]^-$. HRESIMS *m*/*z* 483.1771 $[M + Na]^+$ (calcd for $C_{22}H_{33}ClO_8Na$, 483.1762).

4.16. Chlorovaltrate L (12)

Colorless oil, $[\alpha]_D^{20}$ + 143.6 (*c* 0.45, MeOH); UV (MeOH) $_{max}$ (log ε) 200 (4.12), 254 (3.82) nm; IR (KBr) $_{max}$ 3446, 2963, 1735, 1640, 1614, 1430, 1370, 1195, 1101 cm^{-1}; for ^1H NMR (Me_2CO-d_6, 600 MHz) and ^{13}C NMR (Me_2CO-d_6, 150 MHz) spectroscopic data, see Tables 5 and 6; ESIMS *m*/*z* 539 $[M + Na]^+$ and 551 $[M + Cl]^-$; HRESIMS *m*/*z* 539.2030 $[M + Na]^+$ (calcd for $C_{25}H_{37}ClO_9Na$, 539.2024).

4.17. Chlorovaltrate M (13)

Colorless oil, $[\alpha]_D^{20}$ + 227.3 (*c* 0.59, MeOH); UV (MeOH) $_{max}$ (log ε) 200 (4.10), 255 (3.82) nm; IR (KBr) $_{max}$ 3461, 2963, 1736, 1641, 1612, 1429, 1370, 1245, 1148, 1022 cm^{-1}; for ^1H NMR ($CDCl_3$, 600 MHz) and ^{13}C NMR ($CDCl_3$, 150 MHz) spectroscopic data, see Tables 5 and 6; ESIMS *m/z* 539 $[M + Na]^+$ and 551 $[M + Cl]^-$; HRESIMS *m/z* 539.1676 $[M + Na]^+$ (calcd for $C_{24}H_{33}ClO_{10}Na$, 539.1660).

4.18. Chlorovaltrate N (14)

Colorless oil, $[\alpha]_D^{20}$ + 142.0 (*c* 0.15, MeOH); UV (MeOH) $_{max}$ (log ε) 201(4.12), 254 (3.83) nm; IR (KBr) $_{max}$ 3467, 2962, 1738, 1639, 1612, 1428, 1366, 1230, 1101 cm^{-1}; for ^1H NMR (Me_2CO-d_6, 600 MHz) and ^{13}C NMR (Me_2CO-d_6, 150 MHz) spectroscopic data, see Tables 5 and 6; ESIMS *m/z* 495 $[M + Na]^+$ and 507 $[M + Cl]^-$; HRESIMS *m/z* 495.1769 $[M + Na]^+$ (calcd for $C_{23}H_{33}ClO_8Na$, 495.1762).

4.19. Chlorovaltrate O (15)

Colorless oil, $[\alpha]_D^{20}$ + 226.0 (*c* 0.18, MeOH); UV (MeOH) $_{max}$ (log ε) 201 (4.13), 254 (3.84) nm; IR (KBr) $_{max}$ 3455, 2961, 1737, 1642, 1610, 1432, 1369, 1291, 1110 cm^{-1}; for ^1H NMR (Me_2CO-d_6, 600 MHz) and ^{13}C NMR (Me_2CO-d_6, 150 MHz) spectroscopic data, see Tables 5 and 6; ESIMS *m/z* 439 $[M + Na]^+$ and 451 $[M + Cl]^-$; HRESIMS *m/z* 439.1514 $[M + Na]^+$ (calcd for $C_{20}H_{29}ClO_7Na$, 439.1500).

4.20. Basic Hydrolysis of Chlorovaltrate N (14)

To a solution of **14** (9.0 mg) in THF (2.0 mL) and H_2O (6 mL) was added NaOH (120 mg), and then the mixture was stirred at room temperature for 1 h. After neutralization with 4 N HCl, the solution was evaporated under reduced pressure to give a residue. The later was resolved by Sephadex LH20 chromatography eluting with petroleum ether$CHCl_3$–MeOH (5:5:1) and then preparative TLC using $CHCl_3$–MeOH (25:1) as developing solvent to yield (*R*)-3-methylvaleric acid (1.5 mg): colorless oil, $[\alpha]_D^{20}$ – 6.3 (c 0.15, CH_2Cl_2); ^1H NMR ($CDCl_3$, 600 MHz) δ 2.34 (1H, m, H-2a), 2.15 (1H, m, H-2b), 1.89 (1H, m, H-3), 1.43 (1H, m, H-4a), 1.17 (1H, m, H-4b), 0.90 (3H, t, *J* = 7.2 Hz, H_3-5), 0.96 (3H, d, *J* = 6.6 Hz, H_3-6); ^{13}C NMR ($CDCl_3$, 150 MHz) δ 180.2 (C, C-1), 41.2 (CH_2, C-2), 31.7 (CH, C-3), 29.2 (CH, C-4), 11.2 (CH_3, C-5), 19.2 (CH_3, C-6); ESIMS *m/z* 139 $[M + Na]^+$.

4.21. Cells, culture conditions, and cell proliferation assay

Lin et al. (2009). Pseudolaric acid B was used as a positive control.

Acknowledgments

We acknowledge the Pharmaceutical Analysis Center of Second Military Medical University for measuring the IR and NMR spectra. We also thank the Shanghai Institute of Materia Medica, Chinese Academy of Sciences for the optical rotation determination. The work was supported by program NCET Foundation, NSFC (30725045), partially supported by Global Research Network for Medicinal Plants (GRNMP) and King Saud University, Shanghai Leading Academic Discipline Project (B906), FP7- PEOPLE-IRSES-2008 (TCMCANCER Project 230232), Key laboratory of drug research for special environments, PLA, Shanghai Engineering Research Center for the Preparation of Bioactive Natural Products (10DZ2251300) and the Scientific Foundation of Shanghai China (09DZ1975700, 09DZ1971500, 10DZ1971700).

Appendix A. Supplementary data

Supplementary data associated with this article can be found, in the online version, at http://dx.doi.org/10.1016/j.phytochem.2012.08.015.

References

Allard, P.M., Martin, M.T., Tran Huu Dau, M.E., Leyssen, P., Guéritte, F., Litaudon, M., 2012. Trigocherrin A, the first natural chlorinated daphnane diterpene orthoester from *Trigonostemon cherrieri*. Org. Lett. 14, 342–345.

Becker, H., Chavadej, S., Thies, P.W., Finner, E., 1984. Die Struktur neuer valepotriate aus colchicinbehandelten zellkulturen von *Valeriana wallichii*. Planta Med. 44, 245–248.

Belzecki, C., Trojnar, J., Chmielewski, M., 2000. Practical synthesis of (+)-alloisoleucine. Synth. Commun. 30, 2245–2252.

Bounthanh, C., Bergmann, C., Beck, J.P., Haag-Berrurier, M., Anton, R., 1981. Valepotriates, a new class of cytotoxic and antitumor agents. Planta Med. 41, 21–28.

Chlipala, G.E., Tri, P.H., Hung, N.V., Krunic, A., Shim, S.H., Soejarto, D.D., Orjala, J., 2010. Nhatrangins A and B, aplysiatoxin-related metabolites from the marine cyanobacterium *Lyngbya majuscula* from Vietnam. J. Nat. Prod. 73, 784–787.

Cragg, G.M., Newman, D.J., Snader, K.M., 1997. Natural products in drug discovery and development. J. Nat. Prod. 60, 52–60.

Fuzzati, N., Wolfender, J.L., Hostettmann, K., 1996. Isolation of antifungal valepotriates from *Valeriana capense* and the search for valepotriates in crude Valerianaceae extracts. Phytochem. Anal. 7, 76–85.

Gao, H.M., Zehl, M., Kaehlig, H., Schneider, P., Stuppner, H., Banuls, L.M.Y., 2010. Rapid structural identification of cytotoxic bufadienolide sulfates in toad venom from *Bufo melanosticus* by LC-DAD-MS^n and LC-SPE-NMR. J. Nat. Prod. 73, 603–608.

Li, B., Abliz, Z., Tang, M.J., Fu, G.M., Yu, S.S., 2006. Rapid structural characterization of triterpenoid saponins in crude extract from *Symplocos chinensis* using liquid chromatography combined with electrospray ionization tandem mass spectrometry. J. Chromatogr. A. 1101, 53–62.

Lin, S., Shen, Y.H., Li, H.L., Yang, X.W., Chen, T., Lu, L.H., Huang, Z.S., Liu, R.H., Xu, X.K., Zhang, W.D., Wang, H., 2009. Acylated iridoids with cytotoxicity from *Valeriana jatamansi*. J. Nat. Prod. 72, 650–655.

Lin, S., Chen, T., Liu, X.H., Shen, Y.H., Li, H.L., Shan, L., Liu, R.H., Xu, X.K., Zhang, W.D., Wang, H., 2010a. Iridoids and lignans from *Valeriana jatamansi*. J. Nat. Prod. 73, 632–638.

Lin, S., Shen, Y.H., Zhang, Z.X., Li, H.L., Shan, L., Liu, R.H., Xu, X.K., Zhang, W.D., 2010b. Revision of the structures of 1,5-dihydroxy-3,8-epoxyvalechlorine, volvaltrate B, and valeriotetrate C from *Valeriana jatamansi* and *V. officinalis*. J. Nat. Prod. 73, 1723–1726.

Newman, D.J., Cragg, G.M., Snader, K.M., 2003. Natural products as sources of new drugs over the period 1981–2002. J. Nat. Prod. 66, 1022–1037.

Newman, D.J., Cragg, G.M., 2007. Natural products as sources of new drugs over the last 25 years. J. Nat. Prod. 70, 461–477.

Oh, D.C., Williams, P.G., Kauffman, C.A., Jensen, P.R., Fenical, W., 2006. Cyanosporasides A and B, chloro- and cyano-cyclopenta[*a*]indene glycosides from the marine Actinomycete "*Salinispora pacifica*". Org. Lett. 8, 1021–1024.

Stahi, E., Schütz, E., 1980. Extraktion labiler naturstoffe mit überkritischen gasen 4. Mitt.: extraktion der valepotriate aus *Valeriana wallichii*. Planta Med. 40, 262–270.

Stobiecki, M., Staszków, A., Piasecka, A., Garcia-Lopez, P.M., Zamora-Natera, F., Kachilicki, P., 2010. LC-MSMS profiling of flavonoid conjugates in wild Mexican lupine, *Lupinus reflexus*. J. Nat. Prod. 73, 1254–1260.

Tang, Y.P., Liu, X., Yu, B., 2002. Iridoids from the rhizomes and roots of *Valeriana jatamansi*. J. Nat. Prod. 65, 1949–1952.

Thies, P.W., David, S., 1983. 2,9-Dioxa tricyclo [4,3,1,$0^{3,7}$] decane compounds and process of making same. U. S. Patent 4,391,819.

Yang, X.P., Li, E.W., Zhang, Q., Yuan, C.S., Jia, Z.J., 2006. Five new iridoids from Patrinia *rupestris*. Chem. Biodiversity 3, 762–770.

Yu, L.L., Huang, R., Han, C.R., Lv, Y.P., Zhao, Y., 2005. New iridoid triesters from *Valeriana jatamansi*. Helv. Chem. Acta. 88, 1059–1062.

Zhang, W.D., Lin, S., Shan, L., Su, J., Liu, R.H., Li, H.-L., Shen, Y.H., Xu, X.K., 2009. Uses of iridoid compounds extracted from *Valeriana officinalis* as antitumor agents. Faming Zhuanli Shenqing, CN 101444500.

Zhang, W.D., Su, J., Lin, S., Shan, L., Liu, R.H., Li, H.L., Xu, X.K., 2010. Application of iridoid compounds in preparation of medicine for treating ovarian cancer. Faming Zhuanli Shenqing, CN 101829080.